

Elastic electron-neutral interaction measurements in neon at ultralow energies

C. Sol, F. Devos, and J-C. Gauthier

Groupe d'Electronique dans les Gaz, Institut d'Electronique Fondamentale, Laboratoire associé au Centre National de la Recherche Scientifique, Bâtiment 220, Université Paris-XI-91405, Orsay, France

(Received 10 March 1975)

The cross section σ_{MT} for the elastic momentum transfer of electrons with neon atoms in the electron energy range $3 \times 10^{-3} \leq u(\text{eV}) \leq 5 \times 10^{-1}$ has been deduced from measurements of the microwave absorptivity of a transient cryogenic afterglow plasma. A least-squares fit of our experimental data by the modified effective range formula gives a zero-energy scattering length of $(0.24 \pm 0.015) a_0$, where a_0 is the Bohr radius.

I. INTRODUCTION

Measurements of the energy dependence of the elastic cross section for momentum transfer σ_{MT} of electrons in neon at very low electron energies ($u < 0.1$ eV) present many technical difficulties and results are scarce. The most recent and most comprehensive results down to electron energies of 3×10^{-2} eV are those of Robertson¹ using the electron dc swarm technique. Microwave methods, or ac swarm techniques, have been used by Gilardini and Brown,² Chen,³ and Hoffmann and Skarsgard.⁴ At electron energies lower than 3×10^{-2} eV, no experimental results are presently available. Among recent theoretical works on this problem are those of Thompson⁵ and Garbaty and Labahn,⁶ who included in their calculations both charge exchange and polarization effects.

This paper reports the first measurements of the effective collision frequency in neon plasmas down to average electron energies of 3×10^{-3} eV, thus obtaining useful results for the momentum transfer cross section down to 10^{-3} eV. A pulsed microwave interaction technique has been employed in cryogenic afterglow plasmas created in pure neon and helium-neon mixtures to detect the change in the microwave absorptivity as a function of electron temperature. We have used essentially the method and the apparatus which were described in a previous paper by Sol, Boulmer, and Delpech⁷ (SBD). The unfolding of our experimental data was obtained from a fit to the expression of the modified effective-range theory (MERT) given by O'Malley.⁸ The zero-energy scattering length was then deduced and compared to the available experimental and theoretical data.

II. MICROWAVE METHOD

Our experimental system has been described in more detail in Ref. 9 and in the work by SBD. We used high-purity commercial neon and helium-neon mixture (1:9). The temperature of the dis-

charge tube was controlled by a flow of low-temperature helium gas in the inner chamber of the metallic Dewar.¹⁰ The temperature of the plasma tube and waveguide assembly was monitored by calibrated carbon resistors.¹¹ The cryogenic gas flow was adjusted by applying the amplified and detected output voltage of a balanced ac Wheatstone bridge, having the calibrated resistor in one arm, to a small heater immersed in an external liquid-helium container connected to the head of the Dewar. The plasma-tube temperature was adjustable between 25 and 77 °K; the overall temperature difference along the 45-cm-long wave guide was typically 1 °K. Measurements were also possible at room temperature.

Electron densities n_e and electron-heavy particles collision frequencies ν_{eff} were deduced from the phase shift and the attenuation of a low-power sensing microwave at 8.8 GHz. The electron temperature was changed at a selected time in the afterglow by a medium-power (<300 mW) pulsed microwave heating field at 9.2 GHz. In this work, as was done in the work of SBD, the experimental conditions were chosen so as to insure a Maxwellian velocity distribution function for the electrons and a negligible influence of electron-ion collisions¹² on the measurement of the effective collision frequency.

For each neutral temperature T_0 and density n_0 , measurements of ν_{eff} were made at different electron temperatures T_e . The afterglow plasma was created at four different values of T_0 : 295 °K (room temperature), 77 °K (liquid-nitrogen boiling point), 35 and 28 °K. The pertinent afterglow parameters were in the following ranges: (i) for the atomic density, $5 \times 10^{17} \leq n_0 \leq 4 \times 10^{18}$ cm⁻³; (ii) for the electron temperature, $35 \leq T_e \leq 5000$ °K; (iii) for the electron density, $5 \times 10^8 \leq n_e \leq 5 \times 10^{10}$ cm⁻³. At a given electron temperature, the effective collision frequency was always proportional within error bars to the neutral density, as it should be in a perfect gas with only binary collisions.

In previous papers,^{9,12} we have calculated the coefficient relating the electron-temperature increment ΔT_e to the power of the incident heating microwave, taking into account the distortion of the field lines due to the plasma and its container. It was found that ΔT_e was related to the time-averaged value of the electric field inside the plasma by

$$\Delta T_e = \frac{M_0}{6k} \left(\frac{e}{m\omega_h} \right)^2 \bar{E}_{pi}^2, \quad (1)$$

where the bar denotes suitable averaging over plasma volume, M_0 is the neutral atom mass, and ω_h is the radian frequency of the heating field. The relation between the square of the electric field and the incident available power P_i results in the following practical formula:

$$\Delta T_e = KP_i, \quad (2)$$

with

$$K = C \frac{M_0}{6k} \left(\frac{e}{m\omega_h} \right)^2 \frac{120\pi\lambda_g}{ab\lambda_v}, \quad (3)$$

where λ_g and λ_v are the wavelengths corresponding to the angular frequency ω_h , respectively, in the perturbed waveguide and *in vacuo*, and where a and b are the inside dimensions of the guide. The explicit form of the correction factor C which relates the perturbed and unperturbed values of the electric field has been given elsewhere [Eq. (43) of Ref. 12]. As in helium, we have verified the validity of Eqs. (2) and (3) by radiometric electron-temperature measurements in room-temperature neon afterglows.

III. THEORY OF THE EXPERIMENT

The definition of the electron energy scale is of primary importance in cross-section measurements, as mentioned previously (SBD). It is thus necessary to have a very precise control of the

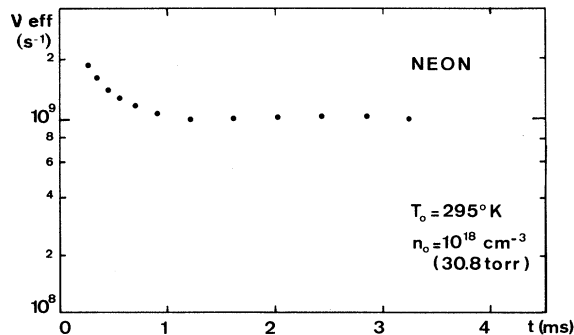


FIG. 1. Experimental variations of the effective collision frequency ν_{eff} with time in a neon afterglow at $T_0 = 295^\circ\text{K}$ and $n_0 = 10^{18} \text{ cm}^{-3}$.

average electron energy (or electron temperature) during the afterglow period.

Figure 1 gives the collision frequencies deduced from the measured microwave absorption in a typical afterglow created in neon at room temperature. The neutral density is equal to 10^{18} cm^{-3} in this case, corresponding to a gas pressure of 30.8 Torr. These measurements were obtained without microwave heating. It can be seen that the collision frequency relaxes rapidly towards a constant value during the afterglow period; simultaneous radiometric measurements, using the technique described in Ref. 13, show this to correspond to the relaxation of the electron temperature to the neutral temperature. At such high neutral density, the random scatter of the points is negligible and the residual slow variations after 1 msec in the collision-frequency measurements shown on Fig. 1 may be attributed to the fact that the reflected power was taken into account to first order only. Such effects have been included in the systematic error bars that we have discussed in the previous work.⁷

Figure 2 shows a log-log plot of the experimental values of the effective collision frequency as a function of the electron temperature T_e for a neutral-gas temperature of 295°K . The collision frequency being linearly dependent on pressure at constant electron and gas temperatures, we have plotted its reduced value at $n_0 = 3.53 \times 10^{16} \text{ cm}^{-3}$. For each electron temperature as measured by the radiometer,¹³ one experimental point was obtained by averaging data at several pressures and at several electron densities. ν_{eff} is seen to vary very nearly with T_e in this particular

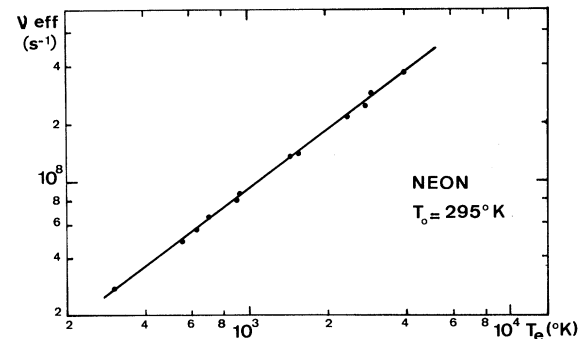


FIG. 2. Collision-frequency measurements reduced to a standard neutral density $n_0 = 3.53 \times 10^{16} \text{ cm}^{-3}$ as a function of the electron temperature. The neutral-gas temperature is 295°K . Each experimental point is the average of several measurements obtained at the same electron temperature and at different electron and neutral densities ($5 \times 10^9 < n_e < 5 \times 10^{10} \text{ cm}^{-3}$; $4 \times 10^{17} < n_0 < 10^{18} \text{ cm}^{-3}$). The solid line with slope unity is a linear fit to the points.

electron-temperature range; this indicates that the collision cross section σ_{MT} is very nearly proportional to the square root of the electron energy.

The interpretation of experimental data such as those presented in Fig. 3 for a neon afterglow at 77 °K is more difficult. The collision frequency does not reach a constant value during the afterglow period accessible to experiment.¹⁴ The measured electron densities are much too low for the variation of the collision frequency with time in the late afterglow to be due to electron-ion collisions.

The experimental situation suggested by these data is in fact very similar to that of helium afterglows at cryogenic temperatures.^{7,9} The slow decrease of the collision frequency may also be explained by a corresponding slow decrease of the electron temperature. Unfortunately, as in the case of helium cryogenic afterglow plasmas, direct radiometric measurement of the electron temperature was not possible, except in the early period of the afterglow. However, if microwave heating is used to produce electron-temperature increments ΔT_e such that the normalized perturbed collision frequency falls in the range covered in Fig. 2, the unperturbed electron temperature may be deduced from the measured data using a limited number of assumptions.

Figure 4 shows the electron density and the collision-frequency evolution when a pulse of microwave heating is applied at 500 μ sec in a neon afterglow at 77 °K ($n_0 = 4 \times 10^{18}$ cm⁻³) for two power levels. The evolution of electron density [see Fig. 4(a)] is qualitatively very similar to the observations we made in a helium afterglow at liquid-helium temperature. These results are equally consistent with the presence of a slowly varying electron-source term in the afterglow. The major difference is that both the electron density and energy-source mechanisms [see Figs. 4(a) and 4(b), after the removal of the heating pulse] are apparently dependent on the time history

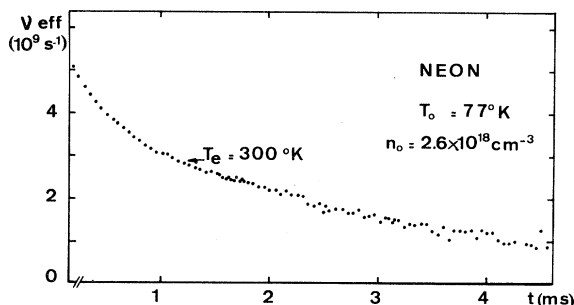


FIG. 3. Experimental variations of the effective collision frequency ν_{eff} with time in the afterglow at $T_0 = 77^\circ\text{K}$ and $n_0 = 2.6 \times 10^{18}$ cm⁻³.

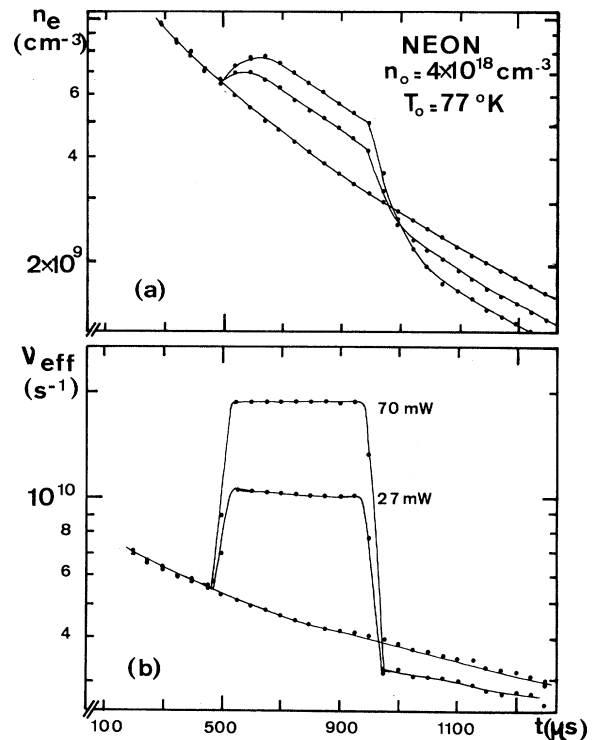


FIG. 4. Variations of the electron density (a) and the effective collision frequency (b) with microwave heating in a neon afterglow at 77 °K ($n_0 = 4 \times 10^{18}$ cm⁻³). The low-power (27 and 70 mW) microwave pulse begins at 0.5 msec; its duration is 1 msec.

of the microwave heating and thus, presumably, of electron density and temperature. Since both the effective collision frequency and the electron density following the heating pulse have not returned to the same value which each attained in the absence of heating, we may conclude that a permanent change in the source has occurred. This source mechanism is probably due to the presence of a large population of atomic and/or molecular metastables, slowly decaying with time through neutral collisions or superelastic collisions with an electron. Direct measurements of the $1s_5$ metastable population in a neon afterglow at room temperature have been made by Wisniewski.¹⁵ When a pulse of microwave heating was applied during the afterglow, the metastable density decreased during heating and did not return to its unperturbed value after heating. Our observations (see Fig. 4) are consistent with these results. This fact enables us to assume that the experimental criteria leading to Eq. (1) are particularly well met at the end of the heating pulse. Indeed, Fig. 4 shows that the electron-density and energy-source terms are substantially decreased from their unperturbed values at the end of the heating interval and that they are slowly varying functions of time

during the electron-temperature transient. Denoting, respectively, t_h and t_0 , the time just before and just after the cessation of heating, the electron temperature $T_e(t_0)$ following the microwave-heating pulse may be deduced from the curves shown on Figs. 2 and 4, provided the electron temperature $T_e(t_h)$ is greater than 300 °K, by the following formula:

$$T_e(t_0) = T_e(t_h) - \Delta T_e, \quad (4)$$

where ΔT_e is the computed electron-temperature increment.

The leading assumption in Eq. (4) is that the computed ΔT_e is effectively the electron-temperature increment produced by the microwave-heating pulse. As mentioned at the end of Sec. II, this proves to be experimentally very well verified over a broad range of electron and neutral densities when the neutral-gas temperature is close to room temperature. Figure 2 shows also that the effective collision frequency is nearly proportional to the electron temperature when its value is greater than 300 °K. In the same electron-temperature range, this should also be the case at lower neutral temperature if the coefficient K is not a function of T_0 . Experimental plots of $\Delta\nu_{\text{eff}}$ as a function of microwave power (or ΔT_e) should then fall very near straight lines having slopes in good agreement with the computed K coefficient. As a sample, Fig. 5 gives two such experimental plots at neutral temperatures of 77 and 35 °K in neon. For comparison, we have also plotted the straight line which corresponds to the computed value of K [see Eq. (3)]. The good agreement between the calculations and our measurements supports the aforementioned assumption.

This procedure gives a very consistent set of

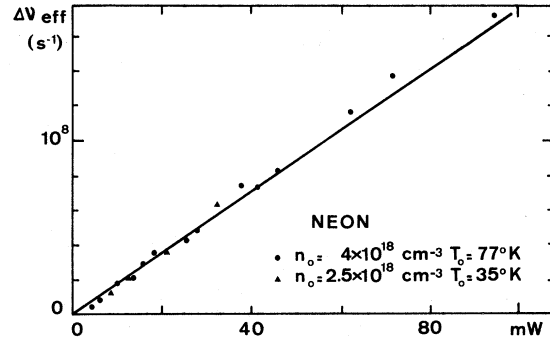


FIG. 5. Typical plot of $\Delta\nu_{\text{eff}}$ as a function of the microwave power at $T_0 = 77$ °K with $n_0 = 4 \times 10^{18}$ cm $^{-3}$ (dots); $T_0 = 35$ °K with $n_0 = 2.5 \times 10^{18}$ cm $^{-3}$ (triangles). The straight line is deduced from Eq. 1.

experimental results when applied to cryogenic temperature afterglows, as we shall see in Sec. IV.

IV. EXPERIMENTAL RESULTS

Figure 6 sums up our experimental results of the effective collision frequency normalized to a neutral density $n_0 = 3.53 \times 10^{16}$ cm $^{-3}$ as a function of the average electron energy. The experimental values were obtained for different gas temperatures ranging from 28 to 300 °K. The scatter of the points is of the order of 5% while systematic errors, as discussed in the work by SBD, are of the order of 7%. The results of Fig. 6 were obtained on a broad range of neutral and electron densities, as discussed in Sec. II; they show no measurable dependence on electron density or on neutral density when the experimental conditions summarized in Sec. II were met.

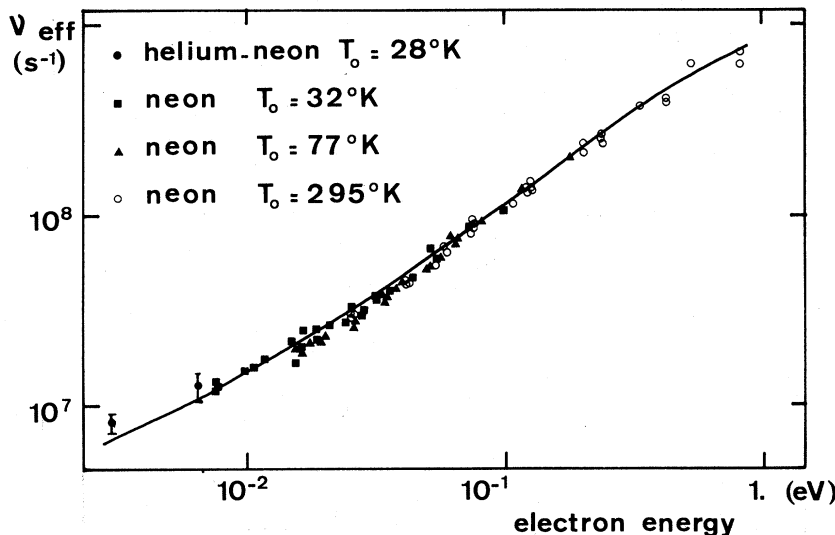


FIG. 6. Summary of our collision-frequency measurements reduced to a standard neutral density $n_0 = 3.53 \times 10^{16}$ cm $^{-3}$ as a function of the average electron energy. The continuous curve is the result of a least-squares fit using the MERT theory.

In pure neon, it was not possible to reach electron energies lower than 8.5×10^{-3} eV even when the gas was cooled down to 28 °K. The mean-electron-energy evolution in the afterglow period is governed by competing processes involving loss terms related to elastic electron-heavy particle collisions and ionization-source terms presumably related to the metastable activity in the afterglow. Loss terms are particularly weak in pure-neon afterglow, owing both to the small value of the elastic electron-neutral collision cross section and to the large neutral to electron-mass ratio. We used a mixture of one part of helium in nine parts of neon to favor energy transfer between electrons and helium atoms so as to increase the influence of loss terms in the energy-balance equation. In the mixture, electron temperatures of 35 °K were attained¹⁶ when the gas was cooled down to 28 °K. The helium contribution of the collision frequency was inferred from the work of SBD and subtracted from the total collision frequency.

The collision frequency is related to the elastic cross section for momentum transfer by Eq. (2) of SBD, our experimental conditions being chosen so as to insure a Maxwellian electron velocity distribution function. The experimental domain of electron energies extends between 3×10^{-3} eV to 1 eV, and it is possible, by inverting the integral equation [Eq. (2)], to get values of the momentum-transfer cross section σ_{MT} on a comparable energy scale. It is easy to see that this problem does not have a unique solution, even if ν_{eff} is known over a large energy range, as in this experiment.

Rather, we have compared directly our experimental results with the available theories and particularly with the MERT theory,⁸ which is particularly well suited for low-electron energies. The momentum-transfer cross section σ_{MT} may be inferred from a limited number of param-

eters using the following expansion:

$$\sigma_{MT} = 4\pi \left(A^2 + \frac{4\pi}{5a_0^2} \alpha A U^{0.5} + \frac{8}{3a_0^3} \alpha A^2 U \ln U^{0.5} \right), \quad (5)$$

where U is the electron energy in Rydbergs (1 Ry = 13.6 eV), a_0 is the Bohr radius ($a_0 = 0.529 \times 10^{-10}$ m), and α is the atom polarizability (for neon we took the currently accepted value $\alpha = 2.65a_0^3$); A is the diffusion length.

The parameter A may be computed from the equation relating the reduced effective collision frequency to the momentum-transfer cross section [Eq. (2) of SBD],

$$\nu_{eff} = \frac{4}{3\pi^{1/2}} \left(\frac{2}{m} \right)^{1/2} \frac{1}{(kT_e)^{5/2}} \times \int_0^\infty \sigma_{MT}(u) u^2 \exp(-u/kT_e) du. \quad (6)$$

Combining Eqs. (5) and (6), we get a polynomial expression for ν_{eff} whose coefficients may be deduced from a least-squares fit to the experimental data. We thus obtain $A = 0.24a_0$. Systematic errors in this quantity are estimated at low electron energies to be less than $\pm 6\%$. In Table I, we compare our result with those of other researchers.

The best fit to our measured collision frequencies is

$$\nu_{eff}(10^{+8} \text{ sec}^{-1}) = 0.66\langle u \rangle^{1/2} + 8.8\langle u \rangle + 0.52\langle u \rangle^{3/2}(\ln\langle u \rangle - 1.36), \quad (7)$$

where $\langle u \rangle$ is the average electron energy measured in eV. When the numerical value of A is entered in Eq. (5), we obtain

$$\sigma_{MT}(10^{-16} \text{ cm}^2) = 0.203 + 1.68u^{1/2} + 0.055u \ln u - 0.144u. \quad (8)$$

Our results are compared in Fig. 7 to those of Robertson,¹ Chen,³ and Hoffmann and Skarsgard.⁴

TABLE I. Summary of theoretical and experimental values of the diffusion length in neon.

References		Nature	Diffusion length (in units of a_0)
Thompson (Ref. 5)	1966	Theory	0.35
Thompson (Ref. 5)	1971	Theory	0.17
MacDowell (Ref. 17)	1971	Theory	0.22
O'Malley (Ref. 8)	1963	Expt. + MERT	0.24
Hoffmann and Skarsgard (Ref. 4)	1969	Expt. + MERT	0.20
Salop and Nakano (Ref. 18)	1970	Expt. + MERT	0.30 \pm 0.03
Robertson (Ref. 1)	1971	Expt. + MERT	0.24
This work	1974	Expt. + MERT	0.24 \pm 0.015

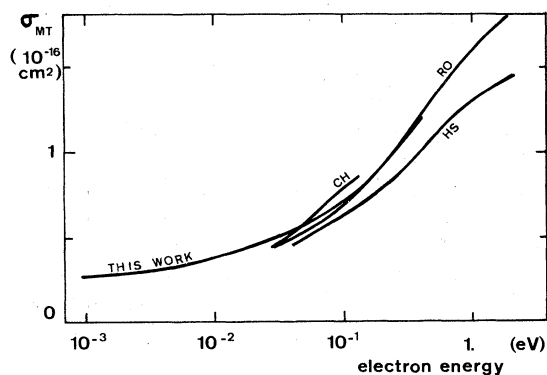


FIG. 7. Electron-neutral-atom momentum-transfer cross section deduced from our collision-frequency measurements. Comparison is made with experimental results of Robertson, Ref. 5 (curve labeled RO); of Chen, Ref. 3 (curve labeled CH); and of Hoffmann and Skarsgard, Ref. 4 (curve labeled HS).

Agreement is quite satisfactory, particularly with the results of Robertson, which we substantially extend in the low-energy limit.

It should be noted that the diffusion length being unambiguously positive, no Ramsauer cross-section minimum should be expected in neon even at very low electron energies.³

ACKNOWLEDGMENTS

It is a pleasure to acknowledge many helpful discussions with Professor L. Goldstein, who suggested this work, and with members of the Groupe d'Electronique dans les Gaz at Orsay, particularly J-F. Delpech and J. Boulmer.

¹A. G. Robertson, *J. Phys. B* **5**, 648 (1972).

²A. Gilardini and S. C. Brown, *Phys. Rev.* **105**, 31 (1957).

³C. L. Chen, *Phys. Rev.* **131**, 2550 (1963).

⁴C. R. Hoffmann and H. M. Skarsgard, *Phys. Rev.* **178**, 168 (1969).

⁵D. G. Thompson, *Proc. Roy. Soc. A* **294**, 160 (1969); *J. Phys. B* **4**, 468 (1971).

⁶E. A. Garbaty and R. W. Labahn, *Phys. Rev. A* **4**, 1425 (1971).

⁷C. Sol, J. Boulmer, and J-F. Delpech, *Phys. Rev. A* **7**, 1023 (1973).

⁸J. F. O'Malley, *Phys. Rev.* **130**, 1020 (1963).

⁹J-F. Delpech and J-C. Gauthier, *Phys. Rev. A* **6**, 1932 (1972).

¹⁰C. Sol, Thèse de Doctorat d'Etat (Orsay, 1972) (unpublished).

¹¹E. H. Schulte, *Cryogenics* **6**, 321 (1966).

¹²J-F. Delpech, J. Boulmer, and J. Stevefelt, in *Advances in Electronics and Electron Physics*, edited by L. Marton (Academic, New York, to be published), Vol. 39.

¹³J-F. Delpech and J-C. Gauthier, *Rev. Sci. Instrum.* **42**, 958 (1971).

¹⁴This period of time is usually of the order of a few milliseconds in our experiment; it is defined as the time scale over which measurable plasma absorptivity is present.

¹⁵E. E. Wisniewski, Ph. D. thesis (University of Illinois, 1971) (unpublished).

¹⁶J-C. Gauthier, Thèse de Doctorat d'Etat (Orsay, 1974) (unpublished).

¹⁷M. R. C. MacDowell, *J. Phys. B* **4**, 1648 (1971).

¹⁸A. Salop and H. H. Nakano, *Phys. Rev. A* **2**, 127 (1970).